Facile Prepared Fe_3O_4 Nanoparticles as a Nano-Catalyst on photo-Fenton process to remediation of methylene blue dye from water: Characterisation and Optimization

Ahmed Halfadji [1,2,*], Mohamed Naous[2], Khaldia nadia Kharroubi[3], Fatima el zahraà Belmehdi[3], and Hanane Aoudia[2]

[1] *Synthesis and Catalysis Laboratory, Ibn Khaldoun University of Tiaret, Tiaret, 14000, Algeria.*

[2] *Department of Sciences and Technology, Faculty of Applied Sciences, Ibn Khaldoun University of Tiaret, Tiare, 14000, Algeria*

[3]*Departement of Chemistry, Ibn Khaldoun University of Tiaret, Tiaret, 14000, Algeria.*

[*]Corresponding author:

E-mail: **e-mail: ahmedhalfadji@gmail.com*, tel: +213656505576.

GRAPHICAL ABSTRACT

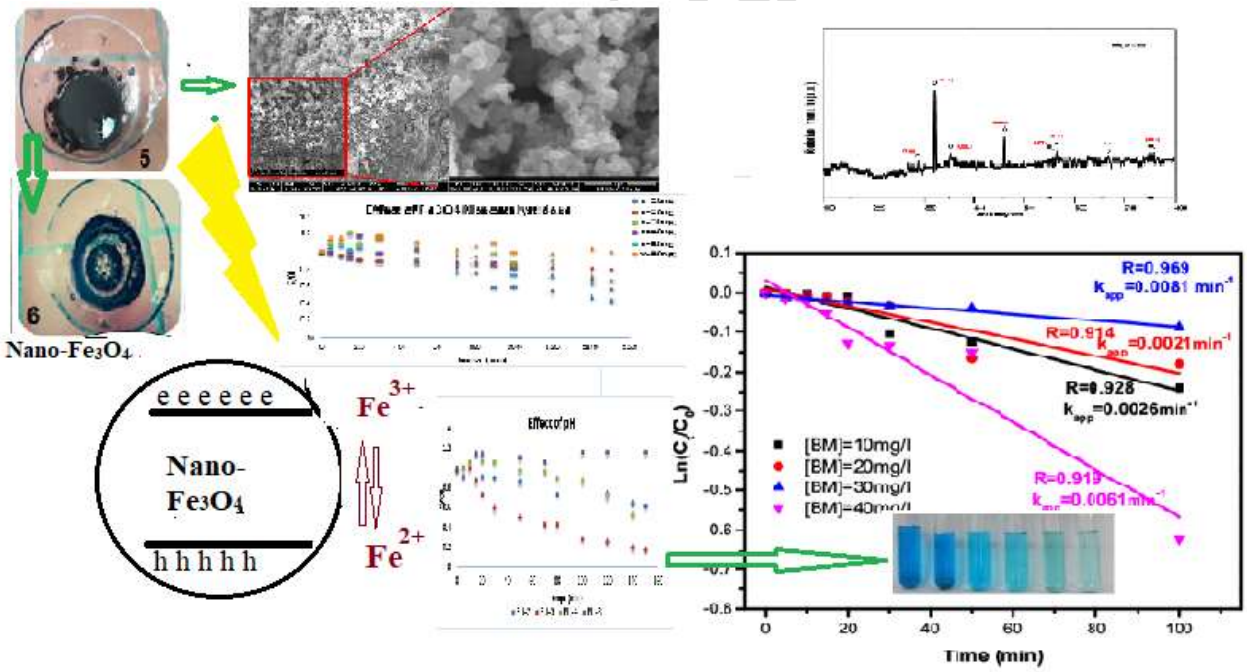

ABSTRACT

In this research, a simple method for the preparation of Fe_3O_4 nanoparticles (Fe_3O_4NPs) with an average size of 38.05 nm via co-precipitation was investigated. X-ray diffraction (DRX), scanning electron microscopy (SEM), and infrared spectroscopy (FT-IR) were used to characterize obtained Fe_3O_4 nanoparticles. These Fe_3O_4NPs were then used as nano-catalysts to degrade Methylene Blue (MB) in an aqueous solution via the Photo Fenton-like process. Also, under room solar light and low temperature, the photocatalytic activity of Fe_3O_4NPs for degrading MB was optimized through various experimental factors such as pH (ranging from 2 to 8), H_2O_2 concentration (from 10^{-2} to 5×10^{-1}M), catalyst amount (20 to 60 mg), and target organic compound concentrations (10 to 40 mg/L). The optimal experimental conditions were found to be a pH of 3, H_2O_2 (0.5M) , a dye concentration of 40 mg/L, and 40 mg of Fe_3O_4NPs as nano-catalyst. These conditions led to a high degree of removal (>86%) of MB dye from water. The pseudo-second-order kinetic model was the suitable model to describe the degradation of MB dye with a coefficient value of 0.969. From this, it was concluded that Fe_3O_4NPs could act as an effective nano-catalyst for a sustainable and environmentally friendly way to eliminate organic pollutants in water and wastewater.

Keywords: Fe_3O_4Nps, structural characterization, MB degradation, photo-Fenton Oxidation process, pseudo-first-order Model, Nanocatalyst.

1. Introduction

Contamination of water with organic pollutants is a significant environmental problem that has negative impacts on both ecosystems and humans. Chemicals such as pesticides, herbicides, petroleum, and dyes are often released into water and wastewater through industrial and agricultural practices (Chowdhary et al. 2020).

Organic pollutants are harmful to aquatic life, the food chain, and water quality. They can also cause health problems for humans, such as cancer and neurological damage (Okoye et al. 2022). Therefore, the treatment of organic contaminated water and wastewater is crucial. Additionally, water scarcity due to drought has been a global issue in recent years. Thus, reusing treated wastewater is an effective approach to conserving freshwater resources (Manikandan et al. 2022). However, before releasing wastewater into the environment or using it for human consumption or agricultural irrigation, it must undergo treatment using methods such as filtration, bioremediation, and chemical treatments (Kesari et al. 2021). These methods aim to remove or degrade pollutants to ensure human safety and maintain the health and sustainability of the ecosystem (Kesari et al. 2021). Industrial activities are a significant source of organic pollutants. The textile industry, in particular, uses numerous organic compounds and dyes, which are discharged as effluent during dyeing and finishing processes. These organic dyes have low biodegradability, thus leading to the long-term pollution of water sources (Kesari et al. 2021). This contamination poses a threat to ecosystems and human health.

The photo-Fenton degradation process is a powerful technique for treating contaminated water, It is an advanced oxidation process (AOP) category, which involves the use of catalysts (materials) to generate highly reactive hydroxyl radicals to degrade pollutants in water and wastewater under light irradiation (Pandis et al. 2022). One of the advantages of this process are highly effective in removing various types of pollutants from wastewater, including organic and inorganic compounds. this process is considered a low-cost technology that does not require expensive reagents or complex equipment. it can be operated at ambient temperature and pressure conditions. also, this process does not generate

toxic by-products and can significantly reduce the amount of sludge generated during the treatment process [(Zhang et al. 2019b). However, this process has disadvantages as the catalyst used can be deactivated over time due to fouling or poisoning by pollutants, which reduces the efficiency of the process. also, this process is highly dependent on optimizing various parameters involved such as the pH of the media, and the nature of catalysts used, This process may not be suitable for the treatment of certain emergent contaminates with high concentrations (Zhang et al. 2019b).

Recently, a heterogenous Fenton-like process also gets considerable interest in the photodegradation of organic pollutants with high efficiency and environmentally benign operation, by using different types of catalysts, such as copper ferrate ($CuFe_2O_4$) doped with Al for degradation tetracycline (> 95%) (Zhong et al. 2023), $FeCeO_x$ for degradation of sulfamethazine (> 90%) (Liu et al. 2023), Fe_2O_3/TiO_2 supported by montmorillonite and aluminum pillared clays for removal three emerging organic contaminates (triclosan, dichlorophenol, and bisphenol) (100%), ZnO/Fe_2O_3@Gr catalyst explored on mineralization of 58.5% to 92.8% of cationic dye crystal violet (Cardona et al. 2023), Mn_3O_4/λ-MnO_2 which reached 90.6% of mineralization phenol (Xing et al. 2023), modified $CuFeO_2$ for degradation of ofloxacin (94.2%)(Zhang et al. 2023), and $FeMnO_x$ nanocube for degradation of Rhodamine (>98%)(Su et al. 2023). the process based on continually production of $^*OH$ following equations (1 -2): $Fe^{2+} + H_2O_2$ -----→ $*OH + OH^-$ (1) and $Fe^{3+} + H_2O_2$ ------→ $Fe^{2+} + HO_2^* + H^+$(2)

On the other hand, recently promising nanomaterials such as Fe_3O_4, ZnO, and TiO_2 which that characterized by their high surface area, can be improved and reach efficiency on the photodegradation of organic pollutants at the laboratory scale. Also, the using Fe_3O_4 nanoparticles and doped Fe_3O_4 on photocatalytic degradation of carbol fuchsin dye, furacilin, and doxorubicin hydrochloride drugs (Frolova and Sukhyy 2023; Koli et al. 2019; Weng et al. 2018; Zhang et al. 2019a), ZnO nanoparticles as nanocatalyst to remove of 2-Chlorophenol and on the degradation of lignin (Lenka and Badamali 2023; Zyoud et al. 2021), TiO_2 on photocatalytic degradation of tebuconazole (TEB), Congo red, and cefotaxime (Abbood et al. 2023; Gianni et al. 2023; Obaiah et al. 2023).

Based on these findings, in the present study, **i)** a facile method was employed for the synthesis of nanoscale Fe_3O_4 Nps particles, and their structural and morphological characteristics were also investigated, **ii)** additionally, under room sunlight and low temperature, the degradation potential of the obtained Fe_3O_4 NPs was investigated for the removal of Methylene Blue dye from water, **iii)** experimental conditions affecting the degradation process of MB, including pH, the amount of nano-catalyst (Fe_3O_4 NPs), concentration of H_2O_2, and the initial amount of the target compound (MB) were optimized. **iv)** The degradation kinetics of MB dye in the presence of Fe_3O_4 NPs were examined using the pseudo-first-order model. As a result, under ambient conditions, Fe_3O_4NPs demonstrated high photocatalytic efficiency. These results are disclosed in detail in this study.

2. Experimental

2.1.Reagents

All reagents used were of chemical reagent grade with good purification. $FeCl_2$,$4H_2O$ (99%), and $FeCl_3$,$6H_2O$ (97%) were purchased from Sigma Aldrich, Spain. Hydrogen peroxide (H_2O_2, 35%), sodium hydroxide (NaOH, 98%), and hydrochloric acid (HCl, 37%), were obtained from Panreac, Germany with analytical grade. Methylene blue (MB) ($C_{16}H_{18}ClN_3S.\ H_2O$) with a molecular weight of 319.85 g/mol and purity of 98%, which is chosen as the target organic pollutant was supplied by Biochem, Germany.

2.2. Chemical preparation of Fe_3O_4NPs

Fe_3O_4 nanoparticles were prepared by co-precipitation method with some modifications according to Kushwaha & Chauhan, (2023) (Kushwaha and Chauhan 2023). Briefly, 16,25 g of $FeCl_3$,$6H_2O$ and 6,35 g of $FeCl_2$,$4H_2O$ were dissolved into 200 ml of distilled water. After stirring for 1h, chemical precipitation was achieved at a heated temperature of 35 °C under vigorous stirring by adding NaOH (2M) solution. The reaction system keeps at 70°C for 5 h with pH=12. Then, the suspension solution was cooled to room temperature; the precipitates were separated by a permanent magnet and washed

with distilled water until pH neutral. Finally, Fe_3O_4NPs were washed with acetone and dried in the oven at 60-70°C. the chemical reaction can be expressed by (3):

$$Fe^{2+} + 2Fe^{3+} + 8OH^- \rightarrow Fe_3O_4 + 4H_2O \qquad (3).$$

2.3. Structural characterizations of synthesized Fe_3O_4NPs

Nanoparticles and Nanocomposites structures were characterized by X-ray diffractometry (XRD) (Rigaku MiniFlex 600 X-ray diffractometer Model) using Cu-K$^{\alpha}$ radiation in the Bragg angle 2θ range (10-80°) at 40 kV and 35 mA and rate of 0.04 degree in 4 seconds. The broadening was calculated from the (101) diffraction peak and the particle size was estimated from the flowing Scherrer equation (4):

$$D = \frac{0.89\lambda}{\Delta W \cos\theta} \qquad (4)$$

Where: D is the average size of the crystallites, ΔW is the full width at half maxima (DWHM), λ is the wavelength of radiation (CuKα=1.5428 A°), and θ is the peak position (in degrees).

The morphology of particles was observed using a scanning electron microscope (SEM, FEI Quanta 650 FEG). The chemical composition of the synthesized materials was assessed by FT-IR spectroscopy with FTIR-S64 (Alpha Bruker). UV-Vis spectrometry (Shimadzu UV-1650-PC) was used to measure BM dye concentration.

2.4.Photocatalytic process using Fe_3O_4NPs as nano-catalyst

The studies of the BM photodegradation were performed in the batch experiments under environmental conditions (under low temperature and room sunlight irradiation) by implementing a set of 250 mL conical flasks under a stirring rate of 150 rpm at 298 k. The photocatalytic process was conducted by varying different operation conditions, such as the initial concentration of BM (10 - 40 mg/), the concentration of peroxide hydrogen H_2O_2 (0.1 to 1 M), pH was adjusted over the range pH 2-4 using HCl and NaOH (1M), the dosage of nan-catalyst (Fe_3O_4NPs) in range of (0.4 to 1 g/L) and reaction time over 120 min. photocatalysis reactions were carried out with a thermostatic shaker at 120 rpm.

The removal percent of BM (R%) was calculated by using the flowing equation (5):

$$R\% = (\frac{Ct}{C0})x100, \quad (5)$$

where C_0 is the initial BM concentration in the solution (mg L^{-1}), and C_t is the BM concentration at time (t) of the removal process.

3. Results and Discussion

3.1. Structural characterization of Fe_3O_4NPs

3.2.SEM analysis

To assess the morphology and size of the Fe_3O_4 nanoparticles, a scanning electron microscope (SEM) is used. As shown in Figure 1, SEM images were obtained at various magnifications (fig. 1), It is clearly found that Fe_3O_4 nanoparticles are synthesized and crystallization with successfully. The morphology of the synthesized nanocomposite was a magnetite-rich powder with uniformly sized, homogeneously dispersed nanoparticles that had strong agglomeration. The nanoparticles' confirmed diameter ranges from 0.02 to 0.05 µm. Similar nano-sphere morphologies were reported for Fe_3O_4 nanoparticles synthesized via other methods, such as hydrothermal (Daou et al. 2006), sol-gel (Lemine et al. 2012), and Conventional co-precipitation method (Pham et al. 2019).

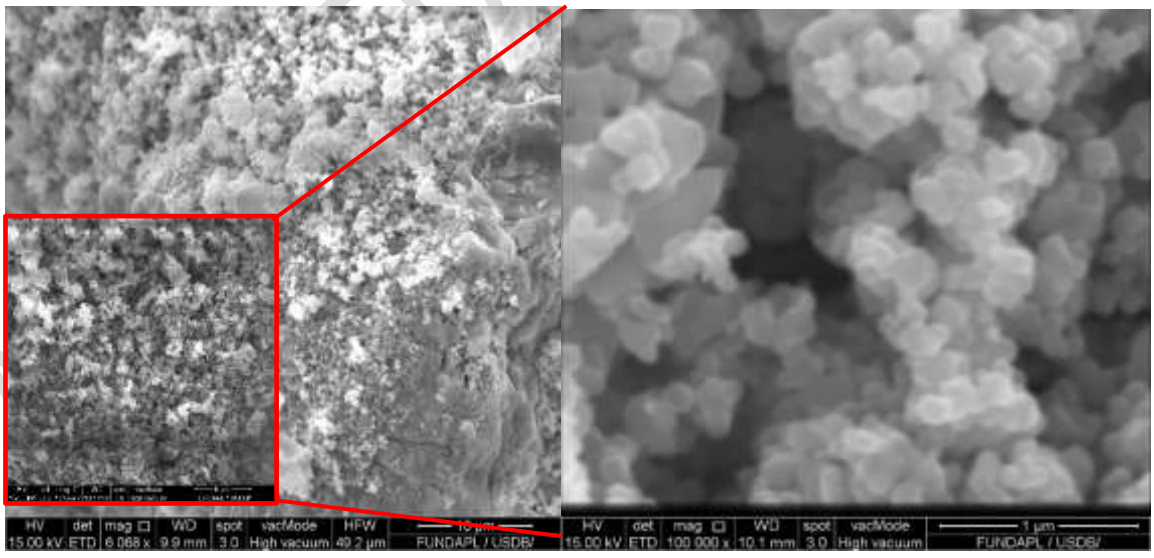

Fig. 1. Scanning electron microscope (SEM) micrographs of the synthesized Fe_3O_4NPs in various magnifications

3.3.FTIR analysis

The structural and chemical properties of the synthesized nanoparticles were determined using the FT-IR spectra. Figure 2 shows FT-IR spectra of Fe_3O_4Nps. As seen, Figure 2 indicates the existence of spectra peaks at 3392 and 1635 cm^{-1}, which correspond to a hydroxyl group (-OH) stretching and bending vibration on Fe_3O_4Nps surface, respectively, as reported in the literature (An et al. 2017; Lezner et al. 2012; Nijpanich et al. 2021; Pucar Milidrag et al. 2022). Additionally, stretching vibrations associated with (-Fe-O-) that were found in the FTIR spectra of Fe_3O_4Nps s at wavelengths of 982, 691, 618, and 511cm^{-1} came from ultrafine magnetite powders (Abbas et al. 2014; Nijpanich et al. 2021; Pucar Milidrag et al. 2022).

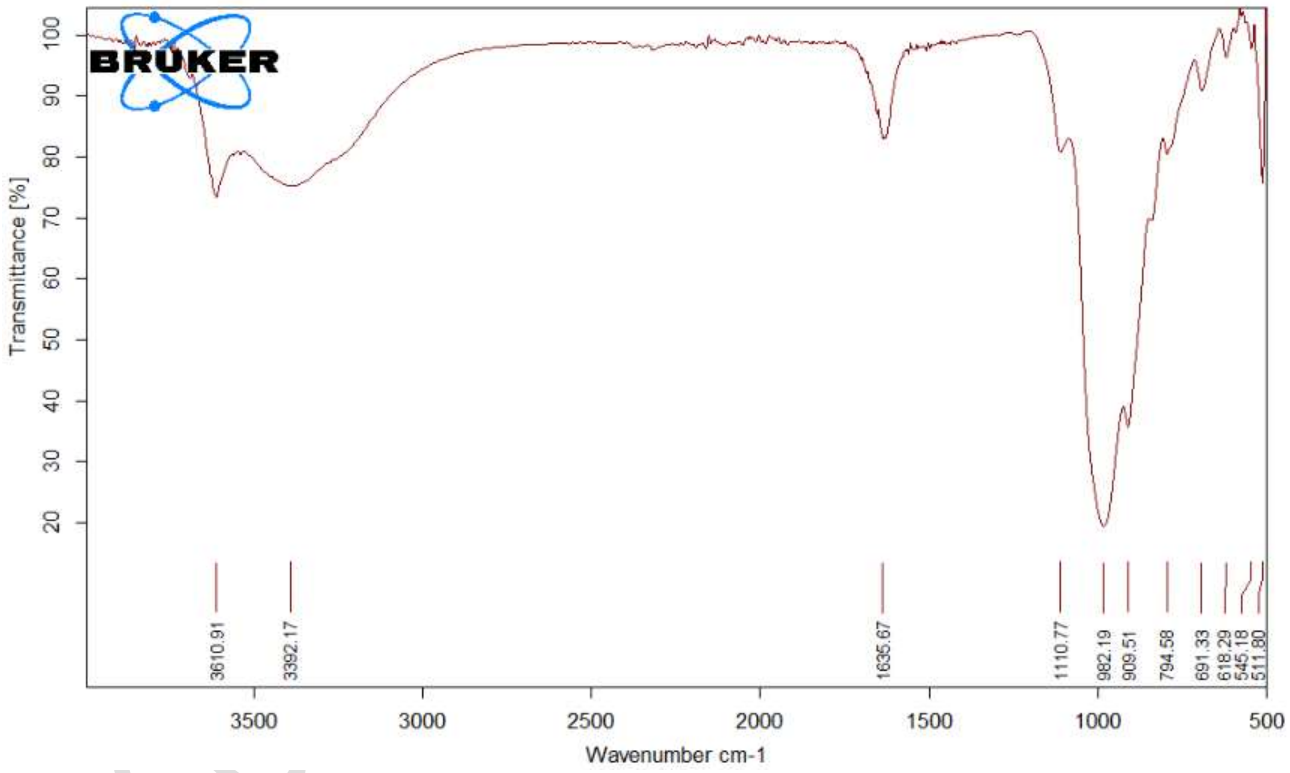

Fig 2. FTIR spectra of synthesized Fe_3O_4Nps.

3.4. X-ray diffraction analysis

The X-ray diffraction (XRD) method is used to determine the products' crystalline phase, phase structure, and crystallite size. XRD results of synthesized Fe_3O_4NPs samples are revealed in Fig 3.

Softwares Match! and X'Petrt High Score are used to treat RDX spectra, and the average crystallite sizes of samples are calculated with the Debye-Scherrer formula.

The diffraction pattern of Fe_3O_4Nps is illustrated in Figure 3, which indicates the major diffraction peaks of Fe3O4NPs are observed at 29°, 32°, 35.5°, 45.1°, 53.4°, 57.0°, 62.33°, and 75.0 °, which correspond to the crystal planes (220), (311), (022), (400), (422), (511), (440), and (533), respectively. These peaks are consistent with the data recorded in reference to JCPDS card No. 19-0629. Additionally, the X-ray peaks of maghemite (210) and (211) are not apparent in the XRD patterns of nanoparticles. The calculated lattice parameters are $\Delta\alpha = 0.5245\pm0.0004$ (JCPDS file 19-629 used for calculation). This result confirmed the cubic inverse spinel structure of Fe_3O_4NPs, which also indicates the successful synthesis of Fe_3O_4 nanoparticles. Also, the XRD of Fe_3O_4NPs reveals that the oxide present is principally magnetite. The average size of Fe_3O_4 nanoparticles calculated according to the Scherrer equation is 38.05 nm.

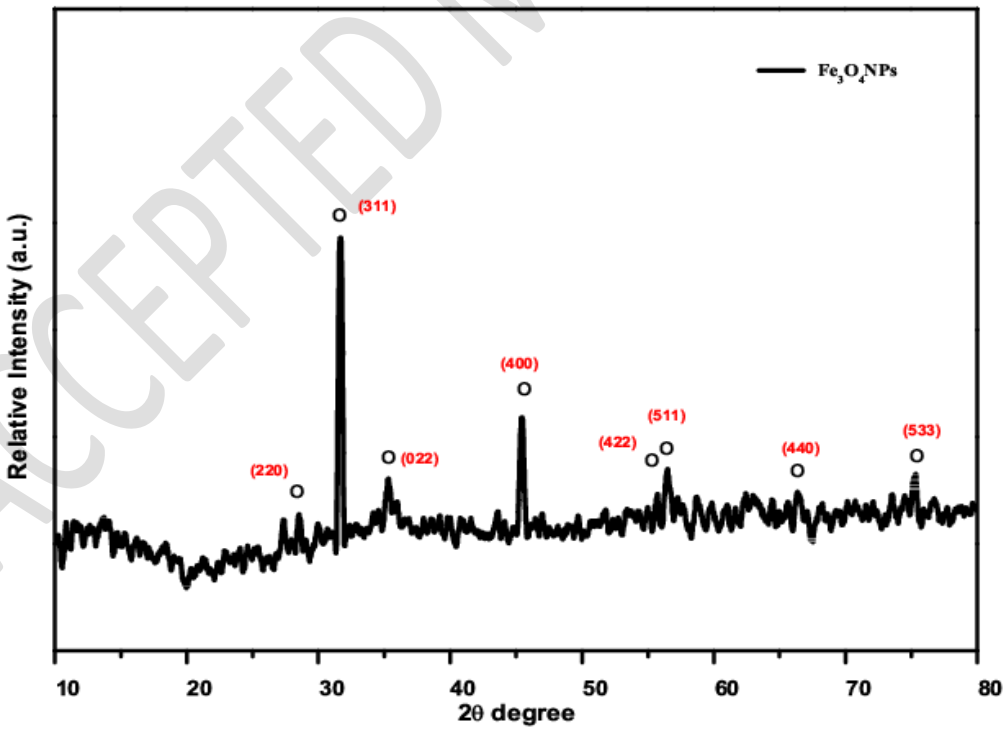

Fig 3. XRD analysis of Fe_3O_4 nanoparticles.

3.5. Photocatalytic activity study of Fe_3O_4NPs

To investigate the photocatalytic degradation of organic pollutants with the nanoparticles under visible light, MB was selected as a model contaminant for photocatalytic decolorization.

In this study, the photocatalytic degradation of BM was investigated using nano-catalysts Fe_3O_4NPs in the presence of H_2O_2 and under visible light, as well as the effect of parameters on the performance of the photo-catalytic process such as solution pH, photo-catalyst dosage, H_2O_2 concentration, and initial dye concentration were evaluated.

3.5.1. Effect of pH

The effects of pH on the photocatalytic activity of BM were investigated. As shown in Figure 4, the efficiency of BM degradation using Fe_3O_4Nps at constant conditions (initial concentration of BM=40 mg/L, duration time of 150 min) is maximum at pH=3 (85 %) and minimum at pH=8 (25 %), indicating the importance of pH value on BM degradation in photocatalytic process under visible light. At acidic pH, Fe_3O_4 nanoparticles can undergo chemical transformations that promote the degradation of MB. For instance, the reduction of Fe^{3+} ions to Fe^{2+} ions is favored in an acidic environment. These Fe^{2+} ions can participate in Fenton-like reactions, generating highly reactive hydroxyl radicals ($^{\bullet}OH$) that are potent oxidants. These hydroxyl radicals can effectively degrade the MB molecules into by products (less toxic compounds).

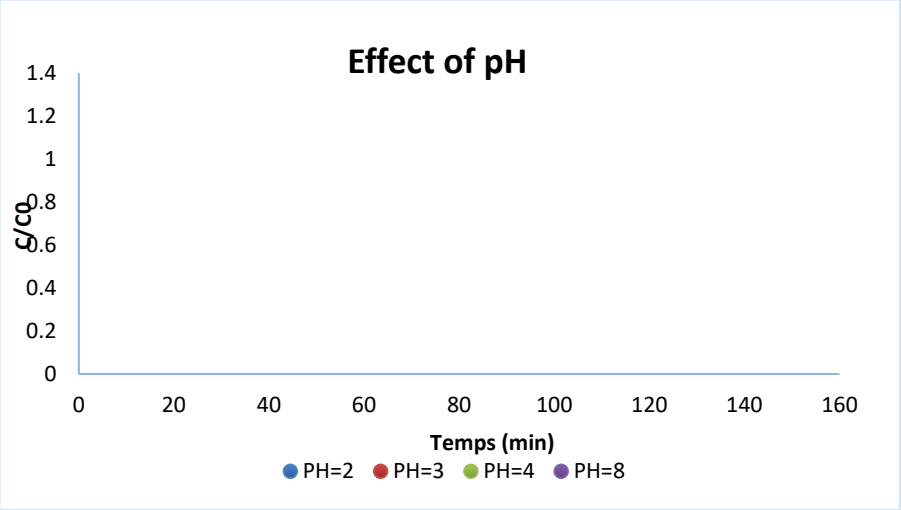

Fig. 4. Effect of pH on photocatalytic removal efficiency of BM using Fe_3O_4Nps

3.5.2. Effect of H_2O_2 Amount

The ·OH radical produced by hydrogen peroxide (H_2O_2) is one of the most effective initiators for increasing fast degradation efficiency. Figure 5 shows the role of H_2O_2 in the degradation of MB using Fe_3O_4NPs in the presence of natural light. The MB dye degradation experiments were carried out with different concentrations of H_2O_2 (30%) in three values: 0.1, 0.5, and 1M. The efficiency of MB degradation was 83% with 0.5 M of [H_2O_2]. We could also see that the degradation is better with concentrations of [H_2O_2]: 1 M, it reaches 75% of the removal rate. For 0.1M we notice a degradation of 60%. This can be explained by the fact that the increase of the H_2O_2 concentration allows the production of a higher quantity of hydroxyl radicals (OH°) and then a massive oxidation of the organic pollutant (Methylene Blue).

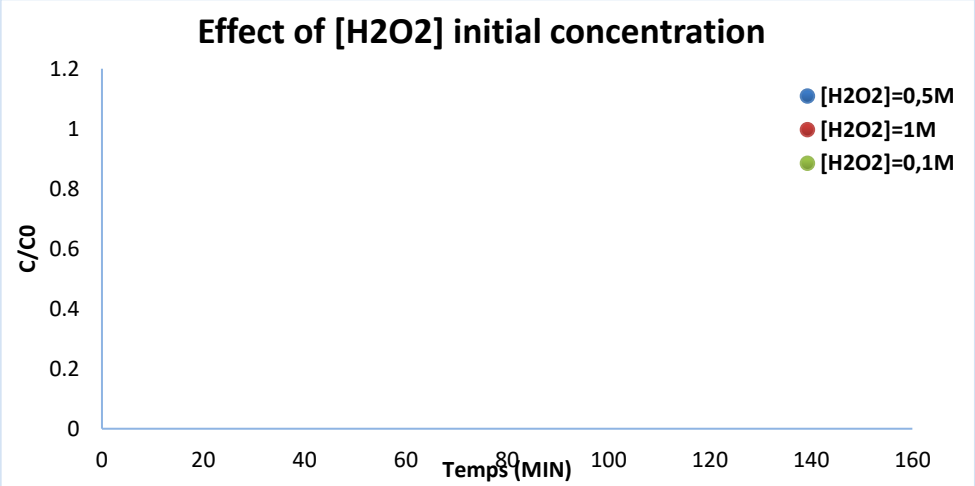

Fig.5. Effect of H_2O_2 concentration for enhanced degradation of MB dye.

3.5.3. Effect of Nano-Photocatalyst (Fe_3O_4NPs) Amount

The effect of Fe_3O_4NPs doses on MB removal was investigated, with photocatalyst amounts ranging from 10 to 80 mg for MB. As shown in Figure 6, increasing the amount of nano-catalyst from 10 to 40 mg increases the MB removal efficiency. However, increasing the nano-photocatalyst amount above 40 mg reduced the removal efficiency, which could be due to decreased light penetration into the solution and increased light dispersion from the surface of nanoparticles (Ebrahimi et al. 2019). As a

result, the optically activated volume decreases, and a small amount of the suspension becomes activated. As a result, 40 mg of nano-catalyst was chosen as the optimum amount.

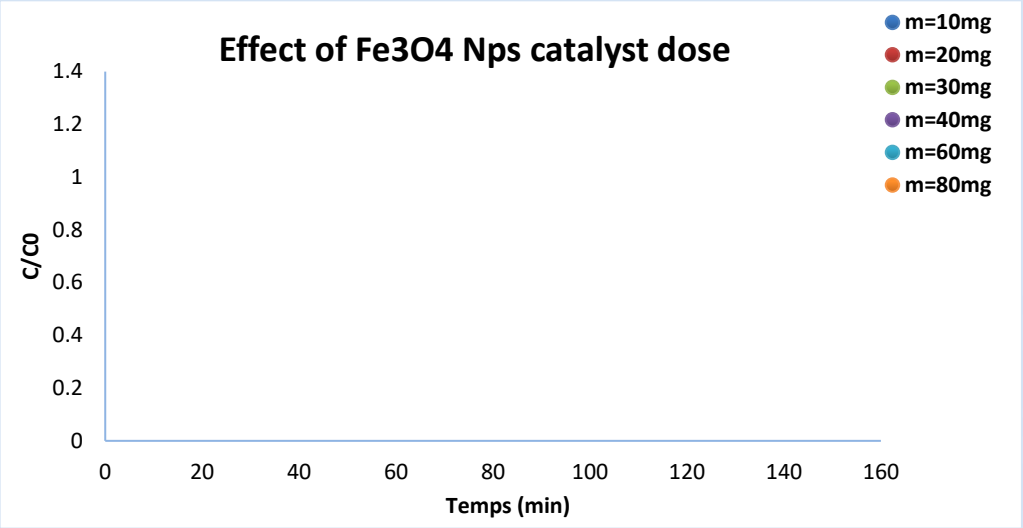

Fig.6. Effect of catalyst mass Fe_3O_4NPs on MB removal

3.5.4. Effect of initial MB concentration

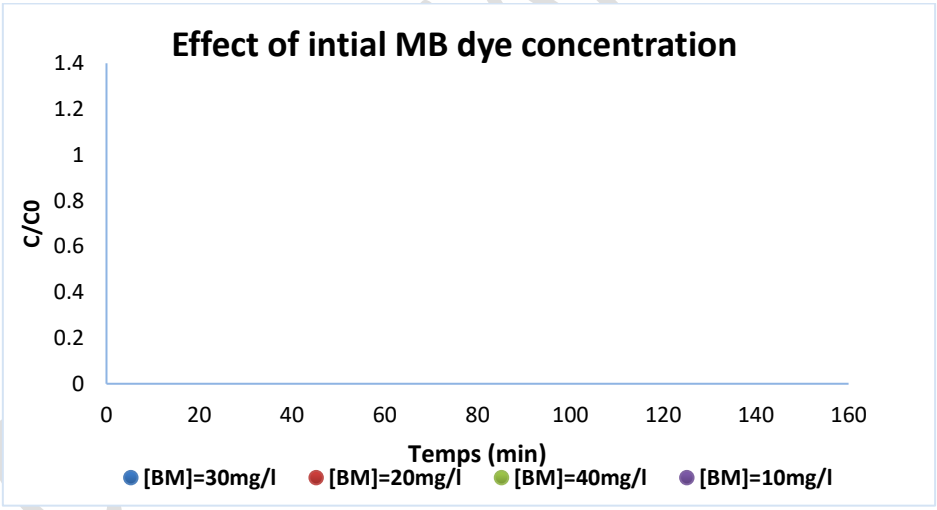

Fig. 7. Effect of MB concentration on degradation process.

The initial concentration of the pollutant is a critical parameter in the photocatalytic degradation of organic pollutants. The effect of initial MB concentration at four different amounts (10, 20, 30, and 40 mg/l) on photo-catalytic degradation was tested at a specific pH value and optimum amount of nano-catalyst, which shows that as the initial concentration of MB increases, the photo-catalytic degradation

process decreases until the 100 min. As shown in Figure 7, the photocatalytic process is more effective at a high MB concentration of 40 mg/l, with 80 % degradation in an exposure duration of 150 min under visible light.

3.6.Kinetic study of degradation MB dye

In order, to evaluate the photocatalytic degradation process of MB dye we applied a pseudo-first-order kinetic model using obtained experimental data. The apparent reaction rate constant ($-k_{app}$) was determined using the first-order reaction model as a flowing equation (6):

$$\ln \frac{Ct}{C0} = -K_{app}.t \qquad (6)$$

Where, two concentrations of pollutants, C_0 and C_t, at initial and at time t (min) of the reaction, respectively, along with a reaction rate constant, k_{app}, which indicates the efficacy of pollutant elimination. The degradation kinetic constants of Fe_3O_4NPs for MB at different concentrations were obtained by first-order kinetic model fitting, indicating that the degradation rate (K_{app}) ranging from 0.021 to 0.0081min^{-1}, and with coefficient $R^2 > 0.91$ for all tested concentrations of MB (Fig. 8).

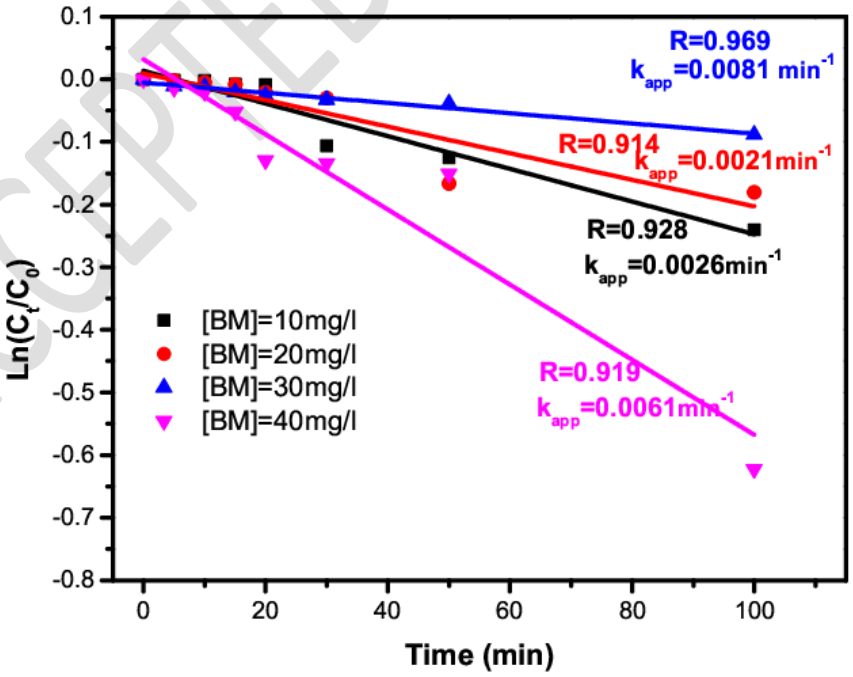

Fig.8. Linearized plots of pseudo-first-order MB decolorization at different concentrations.

4. Conclusions

In this study, we investigated the degradation of Methylene Blue (MB) in aqueous solution using nanocatalysts Fe_3O_4NPs. DRX, FT-IR, and UV-vis were used to characterize their morphology. The Fenton photocatalytic activity of Fe_3O_4NPs to degrade MB was optimized using various experiment factors such as pH (2 to 8), H_2O_2 concentration (0.1 to 1M), amount of nanocomposites catalysts (10 to 80 mg), and MB concentrations. The results show that Fe_3O_4NPs have a high efficiency in degrading BM under the conditions of H_2O_2 (10^{-1}M), catalyst (40 mg), MB (30 mg/L), and pH=3. However, Fe_3O_4NPs have an optimum efficiency under the conditions of H_2O_2 (10^{-1}M), catalyst (40 mg), MB (40 mg/L), and pH=3. Also, the pseudo-second-order kinetic model was found as the best model to describe the photocatalytic degradation of MB. The pH value is an important factor in the efficiency of the oxidation system; in this study, pH=3 demonstrated high efficiencies. The current Photo-Fenton oxidation process using Fe_3O_4NPs as a nano-catalyst can be used as an alternative process to treatment to degrade organic pollutants in water and wastewater.

Conflict of interest

The authors declare that they have no conflicts of interest.

References

Abbas, M., Rao, B. P., Reddy, V., and Kim, C. (2014), Fe3O4/TiO2 core/shell nanocubes: Single-batch surfactantless synthesis, characterization and efficient catalysts for methylene blue degradation., *Ceramics International*, **40**(7), 11177-11186.

Abbood, N. S., Ali, N. S., Khader, E. H., Majdi, H. S., Albayati, T. M., and Saady, N. M. C. (2023). ,Photocatalytic degradation of cefotaxime pharmaceutical compounds onto a modified nanocatalyst., *Research on Chemical Intermediates*, **49**(1), 43-56.

An, X., Cheng, D., Dai, L., Wang, B., Ocampo, H. J., Nasrallah, J., Jia, X., Zou, J., Long, Y., and Ni, Y. (2017). ,Synthesis of nano-fibrillated cellulose/magnetite/titanium dioxide (NFC@ Fe3O4@ TNP) nanocomposites and their application in the photocatalytic hydrogen generation., *Applied Catalysis B: Environmental*, **206**, 53-64.

Cardona, Y., Węgrzyn, A., Miśkowiec, P., Korili, S. A., and Gil, A. (2023). ,Heterogeneous Fenton- and photo-Fenton-like catalytic degradation of emerging pollutants using Fe2O3/TiO2/pillared clays synthesized from aluminum industrial wastes., *Journal of Water Process Engineering*, **52**, 103494.

Chowdhary, P., Bharagava, R. N., Mishra, S., and Khan, N. (2020). ,Role of industries in water scarcity and its adverse effects on environment and human health., *Environmental Concerns and Sustainable Development: Volume 1: Air, Water and Energy Resources*, 235-256.

Daou, T., Pourroy, G., Bégin-Colin, S., Greneche, J.-M., Ulhaq-Bouillet, C., Legaré, P., Bernhardt, P., Leuvrey, C., and Rogez, G. (2006). ‚Hydrothermal synthesis of monodisperse magnetite nanoparticles., *Chemistry of Materials*, **18**(18), 4399-4404.

Ebrahimi, R., Maleki, A., Zandsalimi, Y., Ghanbari, R., Shahmoradi, B., Rezaee, R., Safari, M., Joo, S. W., Daraei, H., and Puttaiah, S. H. (2019). ‚Photocatalytic degradation of organic dyes using WO3-doped ZnO nanoparticles fixed on a glass surface in aqueous solution., *Journal of Industrial and Engineering Chemistry*, **73**, 297-305.

Frolova, L., and Sukhyy, K. (2023). ‚Study of the photocatalytic degradation of furacilin from aqueous solutions using the biochar/Fe3O4 nanocomposite., *Applied Nanoscience*, 1-10.

Gianni, E., Panagiotaras, D., Giannakis, I., Papoulis, D., Bekiari, V., Panagopoulos, G., Petrounias, P., and Kalarakis, A. (2023). ‚Palygorskite-TiO2 nanocatalysts for photocatalytic degradation of Tebuconazole in water., *Water and Environment Journal*.

Kesari, K. K., Soni, R., Jamal, Q. M. S., Tripathi, P., Lal, J. A., Jha, N. K., Siddiqui, M. H., Kumar, P., Tripathi, V., and Ruokolainen, J. (2021). ‚Wastewater treatment and reuse: a review of its applications and health implications., *Water, Air, & Soil Pollution*, **232**, 1-28.

Koli, P. B., Kapadnis, K. H., and Deshpande, U. G. (2019). ‚Transition metal decorated Ferrosoferric oxide (Fe3O4): An expeditious catalyst for photodegradation of Carbol Fuchsin in environmental remediation., *Journal of Environmental Chemical Engineering*, **7**(5), 103373.

Kushwaha, P., and Chauhan, P. (2023). ‚Facile synthesis of water-soluble Fe3O4 and Fe3O4@ PVA nanoparticles for dual-contrast T1-and T2-weighted magnetic resonance imaging., *Magnetic Resonance Imaging*, **95**, 50-58.

Lemine, O., Omri, K., Zhang, B., El Mir, L., Sajieddine, M., Alyamani, A., and Bououdina, M. (2012). ‚Sol–gel synthesis of 8 nm magnetite (Fe3O4) nanoparticles and their magnetic properties., *Superlattices and Microstructures*, **52**(4), 793-799.

Lenka, S., and Badamali, S. K. (2023). ‚Nanostructured ZnO as an efficient heterogeneous photocatalyst towards degradation of lignin under visible light irradiation., *Molecular Catalysis*, **536**, 112918.

Lezner, M., Grabowska, E., and Zaleska, A. (2012). ‚Preparation and photocatalytic activity of iron-modified titanium dioxide photocatalyst., *Physicochemical Problems of Mineral Processing*, **48**(1), 193-200.

Liu, D., Hao, Z., Chen, D., Jiang, L., Wang, J., Cheng, Z., Yuan, C., Cao, Z., Yang, L., and Chen, L. (2023). ‚Enhanced degradation of sulfamethazine in FeCeOx Fenton-like system by tea polyphenols as reducing agents: Performance, mechanism and pathway., *Journal of Environmental Chemical Engineering*, **11**(2), 109563.

Manikandan, S., Subbaiya, R., Saravanan, M., Ponraj, M., Selvam, M., and Pugazhendhi, A. (2022). ‚A critical review of advanced nanotechnology and hybrid membrane based water recycling, reuse, and wastewater treatment processes., *Chemosphere*, **289**, 132867.

Nijpanich, S., Nimpaiboon, A., Rojruthai, P., and Sakdapipanich, J. (2021). ‚Hydroxyl-terminated saponified natural rubber based on the H2O2/P25-TiO2 powder/UVC-irradiation system., *Polymers*, **13**(8), 1319.

Obaiah, G., Gireesha, J., and Mylarappa, M. (2023). ‚Comparative study of TiO2 and palladium doped TiO2 nano catalysts for water purification under solar and ultraviolet irradiation., *Chemistry of Inorganic Materials*, 100002.

Okoye, C. O., Addey, C. I., Oderinde, O., Okoro, J. O., Uwamungu, J. Y., Ikechukwu, C. K., Okeke, E. S., Ejeromedoghene, O., and Odii, E. C. (2022). ‚Toxic chemicals and persistent organic pollutants associated with micro-and nanoplastics pollution., *Chemical Engineering Journal Advances*, 100310.

Pandis, P. K., Kalogirou, C., Kanellou, E., Vaitsis, C., Savvidou, M. G., Sourkouni, G., Zorpas, A. A., and Argirusis, C. (2022). ‚Key points of advanced oxidation processes (AOPs) for wastewater,

organic pollutants and pharmaceutical waste treatment: A mini review., *ChemEngineering*, **6(**1), 8.

Pham, X.-M., Pham, D. L., Hanh, N. T., Dang Thi, T. A., Thuy Giang, L. N., Phuong, H. T., Anh, N. T., Nhung, H. T., Le, G. T., and Hoang, M. H. (2019). ‚An initial evaluation on the adsorption of SO2 and NO2 over porous Fe3O4 nanoparticles synthesized by facile scalable method., *Journal of Chemistry*, 2019.

Pucar Milidrag, G., Nikić, J., Gvoić, V., Kulić Mandić, A., Agbaba, J., Bečelić-Tomin, M., and Kerkez, D. (2022). ‚Photocatalytic Degradation of Magenta Effluent Using Magnetite Doped TiO2 in Solar Parabolic Trough Concentrator., *Catalysts*, **12**(9), 986.

Su, Y., Long, Y., Zhao, S., Wang, P., Xie, F., Huang, J., Han, B., Zhang, Z., and Zhang, B.-P. (2023). ‚Reduced Fe, Mn-based catalyst with dual reaction sites for rapid decolorization treatment via Fenton-like reactions., *Applied Surface Science*, **616**, 156522.

Weng, X., Ma, L., Guo, M., Su, Y., Dharmarajan, R., and Chen, Z. (2018). ‚Removal of doxorubicin hydrochloride using Fe3O4 nanoparticles synthesized by euphorbia cochinchinensis extract., *Chemical engineering journal*, **353**, 482-489.

Xing, Z., Fan, M., Liu, J., Wang, Y., Zhang, X., Li, R., Wang, Y., and Fan, C. (2023). ‚A novel Fenton-like catalyst and peroxymonosulfate activator of Mn3O4/λ-MnO2 for phenol degradation: Synergistic effect and mechanism., *Inorganic Chemistry Communications*, 110396.

Zhang, J., Fan, S., Lu, B., Cai, Q., Zhao, J., and Zang, S. (2019a). ‚Photodegradation of naphthalene over Fe3O4 under visible light irradiation., *Royal Society Open Science*, **6(**1), 181779.

Zhang, L., Huo, S., Li, W., Song, L., Fu, W., Li, J., and Gao, M. (2023). ‚Improved heterogeneous photo-Fenton-like degradation of ofloxacin through polyvinylpyrrolidone modified CuFeO2 catalyst: Performance, DFT calculation and mechanism., *Separation and Purification Technology*, **311**, 123261.

Zhang, M.-h., Dong, H., Zhao, L., Wang, D.-x., and Meng, D. (2019b). ‚A review on Fenton process for organic wastewater treatment based on optimization perspective., *Science of The Total Environment*, **670**, 110-121.

Zhong, W., Peng, Q., Liu, K., Zhang, Y., and Xing, J. (2023). ‚Al3+ doped CuFe2O4 efficiently activates peroxymonosulfate for long-term and stable degradation of tetracycline: synergistic and regulatory role of Al3+., *Separation and Purification Technology*, 123204.

Zyoud, A. H., Salah, H., Zyoud, S. H., Zyoud, S. H., Helal, M. H., Qamhieh, N., Hajamohideen, A., Nassar, H., and Hilal, H. S. (2021). ‚ZnO-based catalyst for photodegradation of 2-chlorophenol in aqueous solution under simulated solar light using a continuous flow method., *JOM*, **73**, 404-410.